Generation of polarization entangled photons using concurrent type-I and type-0 processes in AlGaAs ridge waveguides

Dongpeng Kang and Amr S. Helmy*

The Edward S. Rogers Sr. Department of Electrical and Computer Engineering and the Institute for Optical Sciences,
University of Toronto, 10 King's College Road, Toronto, Ontario M5S 3G4, Canada
*Corresponding author: a.helmy@utoronto.ca

A technique to generate polarization entangled photons using concurrent type-I and type-0 second-order nonlinear processes in monolithic Bragg reflection waveguides is presented and analyzed. Concurrent phase matching is achieved by lithographic tuning of the waveguide ridge width. Nearly perfect entanglement is achievable on-chip through appropriate epistructure design without the need of spectral filtering and group velocity compensation. Theoretical calculations predict that a high quantum interference visibility could be experimentally achieved with the pair generation rate of each process being approximately 3.0×10^6 pairs/s/mW/GHz © 2012 Optical Society of America

OCIS codes: 270.5585, 130.7405, 130.5990, 190.4390.

Entangled photon pairs play a pivotal role in quantum communication and quantum information processing, such as quantum key distribution, quantum teleportation, and dense coding [1]. Spontaneous parametric down conversion (SPDC) using χ^2 nonlinear crystals such as lithium niobate (LN) and potassium titanyl phosphate (KTP) is the most widely used method to generate entangled photon pairs. Periodically poled LN (PPLN) and KTP (PPKTP) waveguides using quasi-phase-matching (QPM) have proven to be the most useful due to the significantly enhanced efficiency they provide. To produce polarization entangled photons from these waveguides, various schemes have been exploited using type-0 and type-I processes in which the pump is TM (V) polarized and the generated photons are copolarized in TM and TE (H) modes, respectively, or type-II process in which the pump is TE polarized whereas the generated photons are cross-polarized in both TE and TM modes [2]. However, all these devices cannot be integrated with pump lasers on the same chip, which is essential for future large-scale quantum information processing. To this end, nonlinear semiconductor waveguides are promising candidates for this task because they can be monolithically integrated with active photonics.

To date, SPDC has been observed in GaAs/AlGaAs waveguides using a counterpropagation scheme [3] and Bragg reflection waveguides (BRWs) [4]. However, no entanglement has been reported using these platforms on chip or off-chip. In principle, polarization entangled photons can be generated using the same methods as those using PPLN or PPKTP waveguides [5,6]. For instance, the Bell states $|\Psi^\pm\rangle = (|H;V\rangle \pm |V;H\rangle)/\sqrt{2}$ can be conventionally produced by a type-II waveguide followed by a beamsplitter (BS). However, the modal birefringence in GaAs/AlGaAs waveguides along with considerable group velocity dispersion (GVD) bring about spectral distinguishability between the cross-polarized photon pairs even if the pump is continuous wave (CW) and thus degrade the quality of entanglement [7]. Although this spectral distinguishability can be removed

by spectral filtering, the pair detection rate would be decreased and the setup complexity would be increased. Moreover, the group velocity mismatch (GVM) between signal and idler photons needs also to be compensated in order to remove the temporal distinguishability. Alternative methods involving type-I or type-0 waveguides to produce the Bell states $|\Phi^\pm\rangle = (|H;H\rangle \pm |V;V\rangle)/\sqrt{2}$ require neither spectral filtering nor group velocity compensation. However, interferometric setups are usually required to separate paired photons, making the systems even more complicated. One solution to simplify the optical setup was demonstrated by Kawashima and coworkers who employed a single PPLN waveguide with a thin-film $\lambda/2$ plate inserted in the middle along the propagation direction [8]. The setup can be further simplified if the considered waveguide can support both type-I and type-0 processes at the same phase matching (PM) wavelength.

In this Letter, we propose and analyze a technique for on-chip generation of polarization entangled photons using concurrent type-I and type-0 processes in an Al-GaAs BRW. Not only does this platform enable the PM of both types by lithographically controlling the ridge width of a BRW, but also allows both schemes to have an identical generation rate through appropriate epitaxial structure design, enabling near-perfect polarization entanglement. This platform is also suitable for monolithic integration with laser pumps and provides a viable route for achieving compact, robust, room temperature electrically pumped polarization entangled photon sources in a chip-form factor.

Recently, type-0, type-I, and type-II second-harmonic generation (SHG) have been observed for the first time in BRWs within a wavelength window as narrow as 17 nm [9]. In principle, polarization entangled photons can be generated by any method using either type-0, type-I, or type-II process as discussed above. However, a superior method, that requires neither group velocity compensation, nor interferometric setups, involves using the type-I and type-0 processes provided that they have the same

© 2012 Optical Society of America

PM wavelength. In order to achieve concurrent PM, modal birefringence at the fundamental wavelength should be cancelled such that the effective indices of the three interacting modes are identical. This can be achieved in ridge waveguides by tailoring the ridge width during the lithography stage. The waveguide structure of this class of devices is schematically shown in Fig. 1. As a representative example, we shall use the epitaxial structure, which was described and characterized in [9] and in the following analysis. The devices in this particular example in [9] have a ridge width of 4.4 μm with PM wavelengths 1550.9 nm for type-I and 1567.8 nm for type-0, with a birefringence of $n_{TE} - n_{TM} \approx 0.0085$. The difference in PM wavelength of the type-I and type-0 processes is 16.9 nm. This PM wavelength difference can be modified by tuning the ridge width given the same etch depth. For this structure, Fig. 2(a) shows that the PM wavelengths of both type-I and type-0 increase as the ridge width decreases. As can be seen from Fig. 2(a), when the ridge width $W = 1508$ nm, both processes are phase matched at $\lambda_{PM} = 1625$ nm. By redesigning the vertical structure, the PM wavelength can be shifted to an arbitrary wavelength, such as 1550 nm. In what follows an optimized design with the PM wavelength around 1550 nm will be demonstrated.

To evaluate the degree of entanglement, we consider the interaction Hamiltonian for the two concurrent SPDC processes in a z-propagating waveguide, where the pump (p) is guided in the TM Bragg mode while the down-converted photon pairs (signal (s) and idler (i)) are co-polarized in TE and TM total internal reflection (TIR) modes as seen in Fig. 1. Using undepleted pump approximation, the interaction Hamiltonian for both SPDC processes is

$$H = \int d\omega_s d\omega_i [\chi_I(\omega_s, \omega_i) a_{TE}^\dagger(\omega_s) a_{TE}^\dagger(\omega_i)$$
$$+ \chi_0(\omega_s, \omega_i) a_{TM}^\dagger(\omega_s) a_{TM}^\dagger(\omega_i)] + H.c., \quad (1)$$

where $a_{TE,TM}^\dagger$ are the mode operators for TE and TM photons and χ_J ($J = I, 0$) is related to the biphoton wave function $\Phi_J(\omega_s, \omega_i) \equiv \alpha(\omega_s + \omega_i) \text{sinc}(\Delta k_J L/2) \exp(-i\Delta k_J L/2)$ and the nonlinear effective area A_{eff}^J by $\chi_J(\omega_s, \omega_i) \propto \Phi_J(\omega_s, \omega_i)/(A_{eff}^J)^{1/2}$, with the waveguide length L, the pump spectral amplitude $\alpha(\omega_s + \omega_i)$, and wave number mismatches Δk_J. Here the effective area of each process is given by the overlap integral as
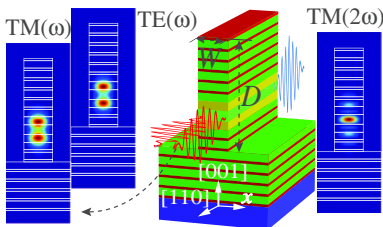

Fig. 1. (Color online) Schematics of the waveguide structure and the modal intensity profiles.
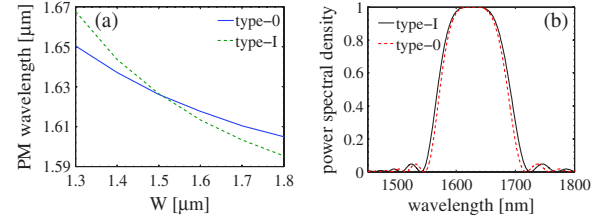

Fig. 2. (Color online) (a) Dependences of type-I and type-0 PM wavelengths on the waveguide ridge width W; (b) the joint power spectral densities using a CW pump.

$$\frac{|\int dx dy d_{ijk} E_i^{(s)*} E_j^{(i)*} E_k^{(p)}|^2}{\int dx dy \epsilon_0 n_p^2 |E^{(p)}|^2 \int dx dy \epsilon_0 n_s^2 |E^{(s)}|^2 \int dx dy \epsilon_0 n_i^2 |E^{(i)}|^2}$$
$$= \bar{d}^2/(A_{eff}^J \bar{n}^6 \epsilon_0^3), \quad (2)$$

where the subscripts i, j, k stand for x, y, z coordinates; d_{ijk} is the nonlinear tensor; E_i is the ith component of the electric field of each mode obtained from a vectorial mode solver; $n_{p,s,i}$ are the refractive index distributions of the three modes; $\bar{d}$ and $\bar{n}$ are the typical values of nonlinearity and refractive index taken to be 50 pm/V and 3, respectively. Note that the values of $\bar{d}$ and $\bar{n}$ do not affect the generation efficiency calculation of each process since all the differences have been grouped into A_{eff}^J [7]. The state, after passing through a 50:50 BS, is polarization entangled and is given by

$$|\Phi\rangle = \frac{1}{N} \int d\omega_s d\omega_i [\Phi_I(\omega_s, \omega_i)/(A_{eff}^I)^{1/2} |H\omega_s; H\omega_i\rangle$$
$$- \Phi_0(\omega_s, \omega_i)/(A_{eff}^0)^{1/2} |V\omega_s; V\omega_i\rangle], \quad (3)$$

where $|;\rangle$ denotes an output state with one photon in each output port, and N is the normalization factor. The minus sign on the r.h.s. is due to the opposite signs of reflection coefficients for H and V polarizations. In obtaining Eq. 3, we neglected terms that represent both photons appearing in the same output port. We used the relation $\Phi_J(\omega_s, \omega_i) = \Phi_J(\omega_i, \omega_s)$, which is true for type-I and type-0 processes. Maximal polarization entanglement requires different photon pairs have the same effective area and biphoton wave function, i.e., $A_{eff}^I = A_{eff}^0$ and $\Phi_I(\omega_s, \omega_i) = \Phi_0(\omega_s, \omega_i)$. These conditions should be taken into account during the design.

Figure 2(b) shows the calculated joint power spectral densities $|\Phi_{0,I}(\omega_s, \omega_i)|^2$ in type-I and type-0 processes using a CW pump for the structure discussed above by taking into account the group velocity and group velocity dispersion of each mode. The high spectral overlap indicates that no or weak spectral filtering is required. The effective areas are calculated to be $A_{eff}^I \approx 32.4$ μm^2 and $A_{eff}^0 \approx 52.0$ μm^2, indicating a maximal degree of entanglement $\gamma \approx 0.789$, with γ defined by $\gamma = \min\{(A_{eff}^I)^{1/2}, (A_{eff}^0)^{1/2}\}/\max\{(A_{eff}^I)^{1/2}, (A_{eff}^0)^{1/2}\}$ [10]. One unique feature of the BRW platform is that it can provide perfect entangled state on chip. Perfect entanglement should be possibly obtained when $A_{eff}^0 = A_{eff}^I$ if the spectral distinguishability is simultaneously satisfied. Therefore, A_{eff}^0 should be decreased and/or A_{eff}^I should be increased. According to Eq. 2, type-0 interaction originates from the E_z components of the TM modes involved, which
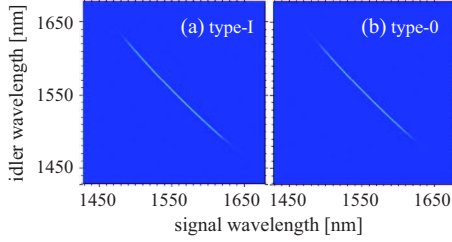
Fig. 3.   (Color online) Normalized power spectral densities for type-I (a) and type-0 (b) using 1.8 ps pump pulses.

are usually negligible in weakly guided waveguides. Meanwhile, the E_z component of a TM mode is proportional to the y derivative of its magnetic field, i.e., $E_z \propto \partial H_x/\partial y$. This means that stronger E_z components and thus smaller A_{eff}^0 could be obtained by increasing the structural variations along the epitaxial direction (y). This can be achieved by increasing the refractive index contrasts between the layers and adjusting the layer thicknesses. The resulting design has a 457 nm $Al_{0.7}Ga_{0.3}As$ core layer surrounded by a 381 nm $Al_{0.2}Ga_{0.8}As$ matching-layer on each side. The bottom and top Bragg mirrors consist of seven and six pairs of 374 nm $Al_{0.25}Ga_{0.75}As$/117 nm $Al_{0.7}Ga_{0.3}As$ respectively. Concurrent PM at 1553.2 nm can be achieved when the etch depth $D = 6\ \mu m$ and ridge width $W = 1347$ nm. The fabrication tolerance could be partly compensated by temperature or electro-optic tuning. The effective areas are calculated to be $A_{eff}^I \approx 33.8\ \mu m^2$ and $A_{eff}^0 \approx 33.3\ \mu m^2$, giving a nearly perfect degree of entanglement $\gamma \approx 1$. The joint power densities for a 2 mm long waveguide using 1.8 ps pump pulses are shown in Fig. 3. The broad bandwidths are not desirable at telecom wavelengths, however, they exhibit a higher spectral overlap and are not much broader than that of a typical type-II AlGaAs waveguide [7].

To better understand the generated state and the quality of its entanglement, we consider the quantum interference visibility of a Bell state test experiment, in which two analyzers oriented at angles θ_1 and θ_2 are placed before the two detectors. Following standard quantum detection theory, the coincidence count rate is given by

$$R_c \propto \int \int d\omega_s d\omega_i \left[\frac{|\Phi_I(\omega_s, \omega_i)|^2}{A_{eff}^I} \cos^2(\theta_1)\cos^2(\theta_2) \right.$$
$$+ \frac{|\Phi_0(\omega_s, \omega_i)|^2}{A_{eff}^0} \sin^2(\theta_1)\sin^2(\theta_2)$$
$$- \frac{2\mathrm{Re}[\Phi_I(\omega_s, \omega_i)\Phi_0^*(\omega_s, \omega_i)]}{(A_{eff}^I A_{eff}^0)^{1/2}}$$
$$\left. \times \cos(\theta_1)\cos(\theta_2)\sin(\theta_1)\sin(\theta_2) \right]. \quad (4)$$

The visibility reaches unity only when $A_{eff}^I = A_{eff}^0$ and $\Phi_I(\omega_s, \omega_i) = \Phi_0(\omega_s, \omega_i)$ are simultaneously satisfied, as dictated by Eq. 4. For the design given above using 1.8 ps pump pulses, the visibility is expected to be 0.95

in the best case, i.e., if no noise originates from the sample in real experiments. This is considerably higher than that which could possibly be obtained from the type-II process in [9], which is lower than 0.6 without spectral filtering. For the technique discussed here, a weak spectral filtering with an bandwidth of 100 nm could increase the visibility to 0.99, enabling nearly perfect polarization entanglement with minimal loss of photon pairs. We stress that such a high visibility could be obtained without group velocity compensation, making the setup considerably simpler.

Another important figure of merit for these devices is the photon pair generation rate. Following the method in [7] which neglects all the losses, the generation rate of both type-I and type-0 processes in the above design is approximately 3.0×10^6 pairs/s/mW/GHz, which is in the same order with the type-II process in [9].

In summary, we developed and analyzed a technique for on-chip generation of polarization entangled photons using concurrent type-I and type-0 SPDC processes in monolithic BRWs. Simultaneous PM is achievable by lithographic tuning of the ridge width in a ridge waveguide. By appropriately designing the waveguide parameters, such as the core thickness and aluminum concentration, we showed that it would be possible to generate maximally entangled photons on chip. We also derived the equation for the coincidence count rate in testing the Bell state experiment and theoretically investigated the achievable visibility. A visibility as high as 0.95 could be obtained using 1.8 ps pump pulses without spectral filtering and group velocity compensation. This result shows a great improvement comparing to existing methods based on type-II process. This platform offers a promising route in realizing electrically pumped devices for on-chip generation of polarization entangled photons.

References
 1. P. Horodecki, M. Horodecki, and K. Horodecki, Rev. Mod. Phys. **81**, 865 (2009).
 2. T. Suhara, Laser Photon. Rev. **3**, 370 (2009).
 3. A. Orieux, X. Caillet, A. Lemaître, P. Filloux, I. Favero, G. Leo, and S. Ducci, J. Opt. Soc. Am. B **28**, 45 (2011).
 4. R. Horn, P. Abolghasem, B. J. Bijlani, D. Kang, A. S. Helmy, and G. Weihs, "A monolithic source of photon pairs," Phys. Rev. Lett. (to be published).
 5. A. Martin, A. Issautier, H. Herrmann, W. Sohler, D. B. Ostrowsky, O. Alibart, and S. Tanzilli, New J. Phys. **12**, 103005 (2010).
 6. T. Zhong, F. N. C. Wong, K. K. Berggren, T. D. Roberts, and P. Battle, Opt. Lett. **35**, 1392 (2010).
 7. S. V. Zhukovsky, L. G. Helt, D. Kang, P. Abolghasem, A. S. Helmy, and J. E. Sipe, Phys. Rev. A **85**, 013838 (2012).
 8. J. Kawashima, M. Fujimura, and T. Suhara, IEEE Photon. Technol. Lett. **21**, 566 (2009).
 9. P. Abolghasem, J. B. Han, B. J. Bijlani, and A. S. Helmy, Opt. Express **18**, 12681 (2010).
10. K. Thyagarajan, J. Lugani, S. Ghosh, K. Sinha, A. Martin, D. B. Ostrowsky, O. Alibart, and S. Tanzilli, Phys. Rev. A **80**, 052321 (2009).